

A guide to characterizing heat release rate measurement uncertainty for full-scale fire tests^{†‡}

Rodney A. Bryant^{*†} and George W. Mulholland

Building and Fire Research Laboratory, National Institute of Standards and Technology, Gaithersburg, MD 20899, U.S.A.

SUMMARY

Accurate heat release rate measurements provide essential information to defining the fire safety characteristics of products. The size, complexity, and cost of full-scale fire tests make achieving accurate and quantitative results a serious challenge. A detailed uncertainty analysis of a large-scale heat release rate measurement facility is presented as a guide to the process of estimating the uncertainty of similar facilities. Quantitative heat release rate measurements of full-scale fires up to 2.7 MW were conducted using the principle of oxygen consumption calorimetry. Uncertainty estimates were also computed for the heat input measurements from a well-controlled natural gas burner. The measurements of heat input and heat release rate were performed independently, and the discrepancy between the two was well within the uncertainty limits. The propagation of uncertainty was performed at the level of voltage and temperature measurements, which avoided using mutually dependent measurement parameters. Reasons for the significant contribution to the combined uncertainty from the oxygen concentration and exhaust flow measurements are demonstrated. Also presented is a first-order effort to account for the uncertainty due to factors in full-scale fire tests such as operator error and environmental influences that are not modeled by the heat release rate equation. Published in 2008 by John Wiley & Sons, Ltd.

Received 22 December 2006; Revised 10 October 2007; Accepted 22 October 2007

KEY WORDS: heat release rate; measurement uncertainty; oxygen consumption calorimetry; fire testing

1. INTRODUCTION

The rate at which heat is released is the single most important quantity in terms of fire safety. Thus, it is important that this measurement be made in a quantitative manner. Heat release is the result of the combustion of a fuel with the oxygen in air. The fuels of primary interest are those found in constructed facilities and include wood, plastics, foam materials used in furnishings (such as polyurethane), wire insulation (such as polyvinyl chloride), and carpet materials (such as nylon).

^{*}Correspondence to: Rodney A. Bryant, Building and Fire Research Laboratory, National Institute of Standards and Technology, Gaithersburg, MD 20899, U.S.A.

[†]E-mail: rbryant@nist.gov

[‡]This article is a US Government work and is in the public domain in the USA.

Heat release rate is a key predictor of the hazard of a fire, directly related to the rate at which heat and toxic gases build up in a compartment or the rate at which they are driven into more remote spaces. Heat release rates on the order of 1 MW to 3 MW are typical in a room that is flashed over or from a single large object such as a bed or sofa.

It is important that heat release rate measurements are accurately conducted because fire regulations can be based on peak rates of heat release. Testing laboratories must be confident that the objects tested pass the required regulation, and manufacturers need accurate information in defining the fire safety characteristics of their products. Another need for accurate heat release rate data is for the development and testing of quantitative models for predicting heat release rate. In comparing a fire experiment and a model prediction, it is essential that the heat release rate measurement have a known uncertainty estimate.

A few studies have addressed the uncertainty of heat release rate measurements by oxygen consumption calorimetry. The studies vary in apparatus, model equation used to compute heat release rate, magnitude of heat release rate, and details of analysis. Axelsson *et al.* [1] estimated the heat release rate measurement uncertainty for the measurement as conducted in the Single Burning Item (EN 13823) and the Room Corner Test (ISO 9705). The uncertainties of the oxygen concentration measurement, followed by the heat of combustion factor and the mass flow rate measurement were identified as the major sources of uncertainty. The study notes that for larger oxygen deficits the combined uncertainty of the heat release rate measurement is less. Sette [2] also conducted an uncertainty analysis on the Single Burning Item Test. The bi-directional probe constant and the measurement of the cross-sectional area of the exhaust duct, both used to compute mass flow rate, were identified as parameters that significantly impact the measurement uncertainty. The study also treats the response time of the measurement facility and asynchronous data acquisition in analyzing the measurement uncertainty with regard to transient effects of the fire. Enright and Fleischmann [3] performed an analytical estimate of the heat release rate measurement uncertainty for the cone calorimeter. The greatest sources of uncertainty identified were the heat of combustion factor, the combustion expansion factor, and the oxygen measurement. Yeager [4] also performed an analytical uncertainty estimate for experiments conducted in a room compartment with a controlled supply of energy into the room and identified the volume flow rate and oxygen measurement as major sources of uncertainty. The oxygen measurement and the heat of combustion factor were also identified as significant sources of uncertainty by Brohez [5], who estimated the uncertainty for the oxygen consumption calorimetry equation corrected for carbon monoxide and soot production.

The oxygen depletion measurement and the exhaust mass flow rate measurement have been consistently reported as major sources of uncertainty. However, Janssens' [6] review of the results of heat release rate round robins brings attention to the uncertainty due to effects such as material and burning variability, environmental conditions, operator error, and measurement bias between laboratories. The impact of these effects is important and deserves further study. However, a crucial first step in such a study is a self-audit by the individual laboratories of their heat release measurement uncertainty using repeatable experiments.

The uncertainty analysis presented here improves upon past investigations to demonstrate in detail why the oxygen concentration and the exhaust flow measurement are significant sources of uncertainty. Also presented is a first-order effort to account for the uncertainty due to factors in full-scale fire test such as operator error, environmental influences, and burning variability that are not modeled by the heat release rate equation. Finally, an example is presented of how the results of the uncertainty analysis serves as a quick reference for estimating the uncertainty over the measurement range of the facility and for establishing a benchmark for quality control purposes.

Such an uncertainty assessment requires the use of a heat input source with good repeatability and therefore documented uncertainty. The goal is to evaluate the calorimetry measurement while avoiding other sources of variability. A well-controlled heat source was used here to conduct experiments to document the uncertainty of a large-scale heat release rate measurement facility. The facility is an open-system with a hood placed above the test object to capture all combustion products and dilution air. It is capable of measuring heat release rates in the range of 0.03 MW to 3.0 MW including brief peaks as high as 5 MW. The well-controlled heat source is a natural gas burner capable of heat release rate up to 8 MW. A detailed description of the heat release rate measurement facility and natural gas burner is presented in Reference [7]. The results of the experiments designed to estimate the measurement uncertainty will be discussed here and are presented as a guide to characterizing and evaluating the performance of large-scale heat release rate measurement facilities.

2. MEASURING HEAT RELEASE

Heat release rate is defined as the sensible enthalpy evolved per unit time as a result of the conversion of the chemical energy of a fuel to heat in a combustion process. Most commonly, the fuel is carbon based and the combustion process is one of oxidation, usually by the oxygen in air. Heat release rate is not directly measured but is inferred from other direct measurements.

For a simple object made from a pure substance with a known constant heat of combustion, the heat release rate measurement requires only a mass loss rate measurement on the object since the former is proportional to the latter, i.e.

$$\dot{q} = \dot{m} \Delta H_c \quad (1)$$

where \dot{q} is the measured rate of heat release, \dot{m} is the mass loss rate (time derivative of decreasing object mass), and ΔH_c is the known lower heat of combustion (e.g. kJ/kg). In practice, the heat of combustion of a complex multi-component object is rarely tabulated and in any case is variable for charring materials. Thus, reliance on mass loss to quantify heat release is unreliable for real objects. On the other hand, mass loss is useful if the 'object' is a well-defined gas or a liquid supplied at a known rate.

In the case of real fuel objects found in living and working spaces, Huggett [8] first suggested the approach, now termed oxygen consumption calorimetry. He followed up on the much earlier finding that the amount of heat evolved from most organic materials per unit mass of oxygen consumed in their complete combustion is nearly constant. Huggett showed that for a wide variety of molecules from pure hydrocarbons, to partially oxygenated species, to partially halogenated species, and a wide variety of polymers and natural materials such as wood and coal, the heat release per unit mass of oxygen falls within a narrow range. He showed that, for most common materials containing C, H, O, and N (hydrocarbons=HC), the average heat produced per unit mass of oxygen consumed, $(\Delta H_c)_{\text{Mass-O}_2}^{\text{HC}}$, is 13.1 MJ/kg O₂; the standard deviation of the heat release rate for materials examined by Huggett is 0.35 MJ/kg O₂. Thus, the oxygen deficit in the duct flow (relative to ambient air) is a measure of the heat release rate in the flow which the duct captures.

Sensenig built the first working apparatus based on oxygen consumption calorimetry [9]. The heat release rate was inferred from the measured oxygen deficit in the flow of a hood that captured

the fire plume as shown in the following equation:

$$\dot{q} = (\Delta H_c)_{\text{Vol-O}_2}^{\text{HC}} \dot{V}_e X_{\text{O}_2}^0 \theta \quad (2)$$

where

$$\theta = (X_{\text{O}_2}^0 - X_{\text{O}_2}) / X_{\text{O}_2}^0 \quad (3)$$

with $X_{\text{O}_2}^0$ being the oxygen volume fraction in the ambient air, X_{O_2} the oxygen volume fraction in the duct after the captured smoke plume (and any excess air) is well mixed, \dot{V}_e is the measured volume flow rate in the exhaust hood, and $(\Delta H_c)_{\text{Vol-O}_2}^{\text{HC}}$ is the average value of heat produced per unit volume of oxygen consumed for a generic fuel (e.g. MJ/m³O₂). This simplified equation is approximate since it neglects other gases that are present such as water vapor and CO₂. The equation does convey, however, the role of the primary variables: duct flow rate and duct oxygen depletion.

Equation (2) assumes complete combustion which may not be the case for practical fires. Oxygen-starved burning, as in flashover conditions, and flame retardants frequently boost CO formation, therefore resulting in incomplete combustion. Often CO formation may exceed 10% of CO₂ formation. In general, it is recommended to measure CO₂ and CO and correct the heat release rate for CO formation. Doing so requires a more thorough treatment of the mass balances (and atom balances) on the species between the fire, where they are generated, and the instruments, where they are measured. This results in an equation of increased algebraic complexity compared with Equation (2).

$$\begin{aligned} \dot{q} = & \left[(\Delta H_c)_{\text{Mass-O}_2}^{\text{HC}} \phi - ((\Delta H_c)_{\text{Mass-O}_2}^{\text{CO}} - (\Delta H_c)_{\text{Mass-O}_2}^{\text{HC}}) \frac{1-\phi}{2} \frac{X_{\text{CO}}}{X_{\text{O}_2}} \right] \\ & \times \frac{\dot{m}_e}{1+\phi(\alpha-1)} (1-X_{\text{H}_2\text{O}}^0) X_{\text{O}_2}^0 \frac{M_{\text{O}_2}}{M_{\text{air}}} \end{aligned} \quad (4)$$

where

$$\phi = \frac{X_{\text{O}_2}^0 (1 - X_{\text{CO}_2} - X_{\text{CO}}) - X_{\text{O}_2} (1 - X_{\text{CO}_2}^0)}{(1 - X_{\text{O}_2} - X_{\text{CO}_2} - X_{\text{CO}}) X_{\text{O}_2}^0} \quad (5)$$

Parker [10] and Parker and Janssens [11] discuss the details of the heat release rate calculation based on the extent to which the duct gas flow is characterized, i.e. whether one measures only oxygen or also includes CO, CO₂, and water. For the experiments discussed here, oxygen, CO₂, and CO were measured and heat release rate was computed using Equations (4) and (5). The derivation is presented in Reference [7].

3. DESCRIPTION OF EXPERIMENTS

A series of experiments were conducted in the NIST Large Fire Research Facility to measure the heat released from a gas burner. The burner simulated the magnitude of the heat release rate from real burning objects. Heat release rate ranged from 0.05 MW to 2.7 MW. Both the heat

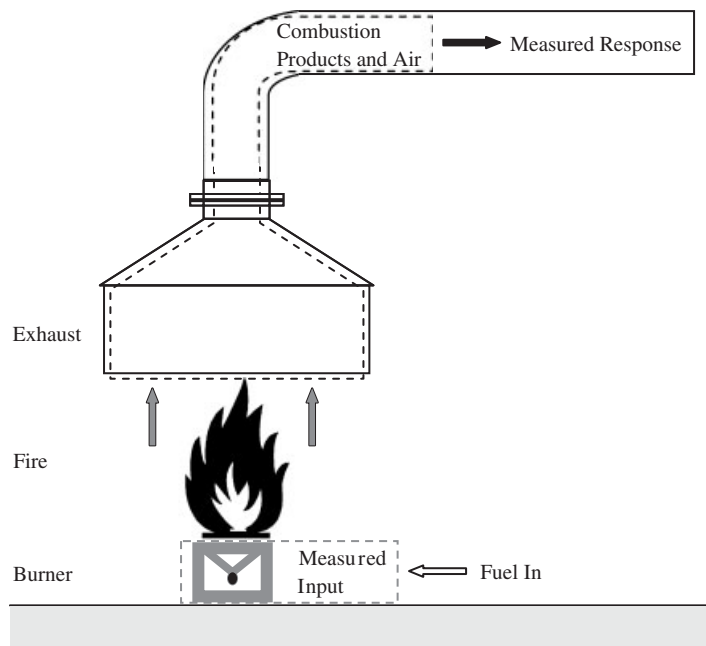


Figure 1. Schematic of the burner that supplied the heat input and the open exhaust system where the response was monitored.

that flowed to the burner and the heat released into the facility exhaust system were independently monitored. The heat released by the process of burning was monitored using the principle of oxygen consumption calorimetry. Figure 1 demonstrates the concept of the two independent measurements: one monitoring the input to the facility and the other monitoring the response of the facility. Details of the burner and the heat release rate measurement facility are discussed in Reference [7].

3.1. Measuring heat input

A precisely controlled gas burner was employed for the purpose of providing a well-known heat input to confirm the calorimetry measurement. The burner and flow system were configured to use natural gas as supplied by the local gas company and having a well-defined heat of combustion. Flow control was performed by a high-precision valve while flow measurement was performed by a rotary volume displacement meter. The ideal heat input was computed from the following equation:

$$\dot{q}_{\text{burner}} = \dot{V}_{\text{NG}} \frac{P}{P_{\text{ref}}} \frac{T_{\text{ref}}}{T} (\Delta H_c)_{\text{NG}} \quad (6)$$

Volumetric flow, temperature, and pressure were measured and the volume flow rate was adjusted to represent the standard conditions for which the heat of combustion was determined. The supplied heat output of the burner ranges from 50 kW to 8 MW. Operation of the burner is automated with control and monitoring integrated into the data acquisition system.

Assuming complete combustion of the natural gas, Equation (6) describes the heat output from the burner and therefore the known input into the heat release rate measurement facility. The process by which the response of the heat release rate facility to the known heat input is measured is, and should be, completely independent of the measurements to monitor the input.

3.2. Measuring heat output

The exhaust systems of the NIST Large Fire Research Facility are equipped to monitor all of the inputs necessary to compute the heat release rate as described by Equations (4) and (5). The systems monitor volume flow rate, oxygen, CO, and CO₂ concentration on a dry basis; a correction is made for ambient humidity or the water concentration in the incoming air. The heat release rate was not corrected for the soot yield. Details concerning the input measurement quantities for Equations (4) and (5) are discussed in Reference [7]. The exhaust system used for this study was capable of measuring heat release in the range of 0.03 MW to 3.0 MW.

Fire tests involving commodities that are designed to burn slowly may require long test periods. Even with the best precautions, it is possible that instruments may suffer significant drift during long test periods. Unfortunately, the instrument drift does not become apparent until the test is completed. Faced with this scenario, the researcher must reduce the occurrence of instrument drift for any subsequent experiments and must also decide whether a repeat test is necessary or whether the data superimposed on instrument drift are salvageable. Because large-scale fire tests are often expensive to conduct and therefore limited in number, salvaging data may be an attractive choice.

Figure 2 is a graphical example of the background value of the heat release rate resulting from the instrument drift during a test. A natural gas burner was employed to deliver a steady heat input at nominal values of 0.05, 0.65, and 2.70 MW. A background drift from 0.005 MW to 0.020 MW was observed over the span of 54 min.

A time-varying relation for the background heat release rate, $\dot{q}_{\text{bgd,sys}}$, relative to which all heat release rate measurements during a test were made, was determined by performing a least-squares linear fit to the data prior to ignition and after the fire was extinguished (in the case of real products, post-data occur after all smoldering is complete), Equation (7). This relation assumes that the background drift of the facility was linear over the entire duration of the fire test. The estimated

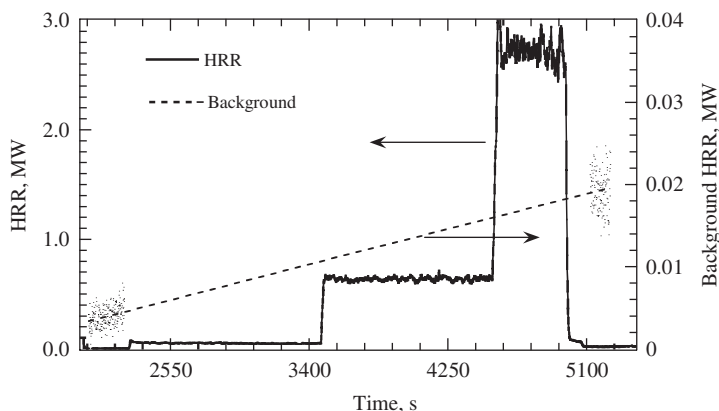


Figure 2. Time history of uncorrected heat release (left axis) and background heat release rate (right axis).

Table I. Background heat release rate comparison.

Background heat release rate (kW)		
$\dot{q}_{\text{bkgd,sys}}$	$\dot{q}_{\text{bkgd,comp}}$	F_d
14.8	11.6	0.22
16.6	12.8	0.23
17.4	11.6	0.26
34.8	35.7	-0.03
39.5	38.8	0.02
51.9	50.2	0.03
55.8	52.1	0.07
65.1	57.1	0.12
	Avg $\pm \sigma$	0.12 \pm 0.10

background heat release rate at time t was algebraically subtracted from the measured value of heat release rate at time t , Equation (8). Performing this operation at each time step resulted in a time history of heat release rate corrected for the background drift of the system, $\dot{q}_{\text{crctd,sys}}$. This operation is especially important when evaluating peak heat release rate. The background will affect the characteristics, such as height and width, of the peak heat release rate curve.

$$\dot{q}_{\text{bkgd,sys}} = m_{\text{sys}}t + j_{\text{sys}} \quad (7)$$

$$\dot{q}_{\text{crctd,sys}} = \dot{q} - \dot{q}_{\text{bkgd,sys}} \quad (8)$$

The method outlined above measures the drift of the system as a whole, $\dot{q}_{\text{bkgd,sys}}$. The system drift is a result of the drift of the system components. Since the raw data from each instrument were recorded, the background heat release rate due to the component drift was also computed. The instruments found to have the most drift were the three gas analyzers (O_2 , CO_2 , and CO). Least-squares linear fits of the voltage outputs of each instrument, Equations (9)–(11), were used to compute the gas species volume fraction implied due to instrument drift. These background volume fractions were substituted into Equation (4) to compute the background heat release rate due to the instrument drift, $\dot{q}_{\text{bkgd,comp}}$

$$V_{\text{O}_2,\text{bkgd}} = m_{V_{\text{O}_2}}t + j_{V_{\text{O}_2}} \quad (9)$$

$$V_{\text{CO}_2,\text{bkgd}} = m_{V_{\text{CO}_2}}t + j_{V_{\text{CO}_2}} \quad (10)$$

$$V_{\text{CO},\text{bkgd}} = m_{V_{\text{CO}}}t + j_{V_{\text{CO}}} \quad (11)$$

A comparison of the values of background heat release rate for the two methods appears in Table I. The fractional difference, F_d , defined as $(\dot{q}_{\text{bkgd,sys}} - \dot{q}_{\text{bkgd,comp}}) / \dot{q}_{\text{bkgd,sys}}$ has an average value of 0.12. This confirms that most of the background heat release rate is due to the drift from the gas analyzers. Note that a background heat release rate of 0.065 MW is 2% of the maximum heat release rate measured in this study. A concerted attempt should be made to eliminate nonzero background values, and, if not eliminated, the measured values should be corrected for the known offset. In addition, the uncertainty analysis must include the correction as demonstrated in Table V.

4. ASSESSMENT OF UNCERTAINTY

A self-audit by individual laboratories of their heat release rate measurement uncertainty is a crucial first step in reducing disagreement in results from laboratory to laboratory in round robin exercises. A burner with good repeatability and documented uncertainty of its measured heat input is recommended in such an audit. The goal is to evaluate how well the measurement facility responds to the burning of a known fuel.

The self-audit conducted here follows the methodology described in the ISO guidelines [12] and adopted by NIST [13]. The approach is to represent each component of uncertainty as a standard uncertainty. The propagation of uncertainty was applied to the equations describing the measured heat input, Equation (6), and measured heat release rate, Equation (4). Each measurement process has an output y and that output y is based on a number of input quantities, x_i

$$y = y(x_1, x_2, x_3, \dots, x_N) \quad (12)$$

In the case that all input quantities are not mutually dependent, the relative expanded uncertainty is given by

$$\frac{U_c(y)}{y} = k \frac{u_c(y)}{y} = k \sqrt{\sum_{i=1}^N s_i^2 \left(\frac{u(x_i)}{x_i} \right)^2} \quad (13)$$

where $u(x_i)$ is the standard uncertainty for each input, $u_c(y)$ is the combined uncertainty, k is the coverage factor, and s_i is the associated dimensionless sensitivity coefficient given by

$$s_i = \frac{\partial y}{\partial x_i} \frac{x_i}{y} \quad (14)$$

The assessment begins with estimating the uncertainty of individual Type A and B components. So-called Type A uncertainties are those that can be computed based on statistics such as the standard deviation about the mean. The others, designated as Type B, require scientific judgment together with available data. A common example is knowing the maximum range of a variable and then converting this range into a standard uncertainty by dividing it by $2\sqrt{3}$ [13].

The nominal values and estimated standard uncertainty of selected parameters are presented in Tables II and V. Nominal values are taken from heat release rate measurements approximately equal to 0.65 MW.

Table II. Nominal values and standard uncertainties of heat input measurement parameters for a nominally 0.65 MW natural gas fire.

Parameter (units)	Nominal value	$u(x_i)/x_i$	Uncertainty type
T (K)	293	0.002	B
P (atm)	2.02	0.005	B
\dot{V} (m ³ /s)	0.0093	0.010	A
$(\Delta H_c)_{\text{NG}}$ (kJ/m ³)	33 733	0.004	A
$\frac{u_c(\dot{q}_{\text{burner}})}{\dot{q}_{\text{burner}}}$		0.012	

4.1. Measured heat input uncertainty

Total rate of heat input into the measurement facility is inferred from three direct measurements: temperature, pressure, and volume flow rate. The relation to compute the heat generated at the natural gas burner, Equation (6), is a multiplicative product of each parameter. Therefore, s_i is unity for each parameter and each parameter's standard relative uncertainty is equally weighted in computing the combined relative uncertainty of the heat input measurement

$$\frac{u_c(\dot{q}_{\text{burner}})}{\dot{q}_{\text{burner}}} = \sqrt{\left(\frac{u(P)}{P}\right)^2 + \left(\frac{u(\dot{V})}{\dot{V}}\right)^2 + \left(-\frac{u(T)}{T}\right)^2 + \left(\frac{u((\Delta H_c)_{\text{NG}})}{(\Delta H_c)_{\text{NG}}}\right)^2} \quad (15)$$

Nominal measurement values for the heat input computation are presented in Table II, along with estimates of standard relative uncertainty. The volume flow rate was the only dynamic variable in this calculation and its contribution to the uncertainty dominates.

4.2. Measured heat release rate uncertainty

The calculation of the uncertainty in the heat release rate measurement requires the combining of many components of uncertainty. This is apparent from the heat release rate equation, Equation (4), which is a function of more than 10 variables. There are four new aspects to the uncertainty analysis presented here compared with previous analyses in the literature. The first is expressing all of the instrument outputs in terms of their voltage or temperature to eliminate correlations induced in intermediate quantities by common measurement results; the benefit is demonstrated in the estimation of the uncertainty in the oxygen volume fraction to take into account the small noise relative to a much larger uncertainty in the calibration gas. A second is including the gas analyzer drift correction in the uncertainty analysis. The third is performing the uncertainty propagation with a numerical method that is easily implemented in a spreadsheet program. And the fourth is attempting to reflect the uncertainty of the measurement process by combining the standard deviation of measurements repeated over a period of time with the combined uncertainty estimated from the uncertainty propagation.

Upon reducing the expression for \dot{q} down to some basic parameters a few levels above the measured voltages and temperatures, it is revealed that the expression contains parameters that are mutually dependent, meaning that they share variables. Pairs such as ambient and depleted oxygen volume fractions, $(X_{\text{O}_2}^0, X_{\text{O}_2})$, and ambient and generated carbon dioxide volume fractions, $(X_{\text{CO}_2}^0, X_{\text{CO}_2})$, are all functions of the zero and span values used in the instrument calibration. Similarly, the gas velocity and temperature measured at each bi-directional probe, $(U_{\text{bdp},i}, T_{\text{bdp},i})$, are mutually dependent since the velocity is computed by making use of the temperature measurement.

Mutually dependent measurements violate the assumption leading to Equation (13). In order to avoid such dependency induced by common inputs, the uncertainty analysis should be performed on the most basic measurement inputs: instrument voltages, thermocouple temperatures, and constant parameters (universal, empirical, and calibration). An example to illustrate the benefit of considering the basic measurements follows.

Consider the volume fraction measurement of a gas, $X_i = (X_S/V_S)V_i$. Its uncertainty is assumed to have two components, the uncertainty in the calibration gas, $u(X_S)$, and the measurement noise, $u(V_i) = u(V_S)$. Two measurements of volume fraction are conducted, X_1 and X_2 , with the same instrument, after a single calibration and at separate times. The algebraic difference in the measurements, ΔX , is the quantity of interest. Figure 3 is a graphical representation of the

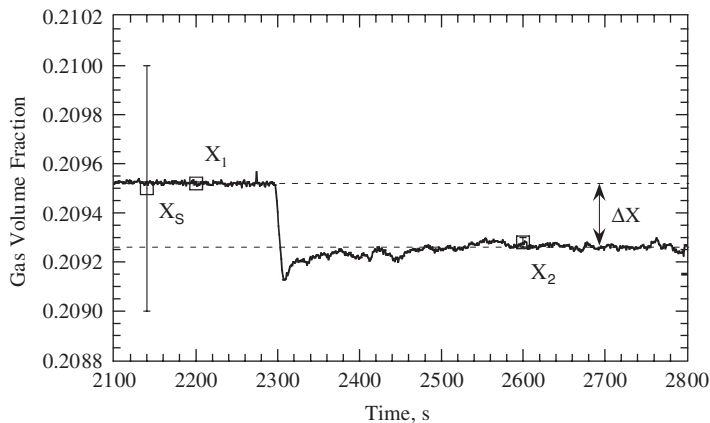


Figure 3. Example of mutually dependent difference measurement.

measurement example. If standard breathing air is used as the calibration gas, $u(X_S)$ (displayed as the error bar at X_S) may be a factor of 20 greater than $u(V_i)$ (displayed as error bars at X_1 and X_2 , these error bars should not be mistaken for $u(X_1)$ or $u(X_2)$, which are much greater). Using the propagation of uncertainty, one obtains the following expression for the combined relative uncertainty for X_1 and X_2 :

$$\frac{u(X_i)}{X_i} = \sqrt{\left(\frac{u(X_S)}{X_S}\right)^2 + \left(\frac{u(V_S)}{V_S}\right)^2 + \left(\frac{u(V_i)}{V_i}\right)^2} \quad (16)$$

To further illustrate the example, the following values are assumed: $X_S = 0.21$, $u(X_S)/X_S = 0.00239$, $V_S = V_1 = 1.0 \text{ V}$, $V_2 = 0.995 \text{ V}$, $u(V_S)/V_S = u(V_1)/V_1 = u(V_2)/V_2 = 0.00003$. Substituting these values into Equation (16), the combined relative uncertainty for both X_1 and X_2 is computed, $u(X_1)/X_1 = 0.00239 = u(X_2)/X_2$. This value is the same as the standard relative uncertainty for the species volume fraction in the calibration gas, therefore demonstrating that the uncertainty of a single volume fraction measurement is dominated by the uncertainty of the calibration gas.

The difference in the species volume fraction is the quantity of interest, $\Delta X = X_1 - X_2$. If the volume fractions are treated as independent measurements, a propagation of uncertainty on the difference would result in the following relation:

$$\frac{u(\Delta X)}{\Delta X} = \sqrt{\left(\frac{X_1}{X_1 - X_2}\right)^2 \left(\frac{u(X_1)}{X_1}\right)^2 + \left(\frac{-X_2}{X_1 - X_2}\right)^2 \left(\frac{u(X_2)}{X_2}\right)^2} \quad (17)$$

Again, by substituting the previous assumed and computed values, the combined relative uncertainty of the difference is computed, $u(\Delta X)/\Delta X = 0.67441$. This is a large uncertainty and it is apparent from Equation (17) that it is dominated by the uncertainty from the calibration gas that propagates through to each volume fraction uncertainty. The uncertainty contribution is also amplified at small differences in volume fraction. This uncertainty estimate would be appropriate in the case of two separate instruments and two separate calibration gases, therefore independent measurements of species volume fraction.

In the present experiments, a single gas analyzer and calibration gas were used to measure oxygen volume fraction. The measurements used to compute the oxygen depletion were separated in time and were therefore mutually dependent. To illustrate how to account for mutually dependent parameters, the volume fraction measurements are expressed in terms of the calibration gas volume fraction, X_S , the voltage of the analyzer corresponding to the calibration gas, V_S , and the voltage corresponding to the gas volume fraction at measurements 1 and 2, V_1 and V_2 . In this case, the difference in the volume fractions is expressed as

$$\Delta X = X_1 - X_2 = \frac{X_S}{V_S}(V_1 - V_2) \quad (18)$$

Carrying out the uncertainty propagation for Equation (18), one obtains the following expression for the uncertainty:

$$\frac{u(\Delta X)}{\Delta X} = \left(\left(\frac{u(X_S)}{X_S} \right)^2 + \left(-\frac{u(V_S)}{V_S} \right)^2 + \left(\frac{V_1}{V_1 - V_2} \frac{u(V_1)}{V_1} \right)^2 + \left(\frac{-V_2}{V_1 - V_2} \frac{u(V_2)}{V_2} \right)^2 \right)^{1/2} \quad (19)$$

Substituting the previous illustrative values, the combined relative uncertainty for the difference in volume fraction is computed, $u(\Delta X)/\Delta X = 0.00880$. This value is almost 77 times smaller than the previous estimate, which was dominated by the uncertainty of the calibration gas. Using the intermediate parameter, volume fraction, and treating the two as independent would have resulted in a serious overestimate of the uncertainty. Equation (19) demonstrates that the uncertainty of the calibration gas (the first term) continues to be important but it is not amplified at very small differences in volume fraction. This amplification occurs more appropriately at the voltage measurements (terms 3 and 4). Equation (19) and Figure 3 also demonstrate the difficulty in making an accurate difference measurement in the presence of signal noise. This example illustrates why it is important that computations accurately reflect the measurement process and why the basic measurements, voltages or temperatures, should be considered when performing an uncertainty analysis.

Reducing the measured heat release rate relation to basic measurements of voltage and temperature will greatly increase the number of measured parameters to track, therefore requiring many partial differentiations in the computation of s_j . Equation (13) will result in an algebraically complex relation that could be handled by a symbolic manipulation program. Alternatively, a spreadsheet program called the Kragten worksheet can be applied to compute the combined uncertainty with equal performance.

The Kragten worksheet numerically approximates all of the partial derivatives and calculates the combined standard uncertainty without the use of intermediate quantities that violate the condition of mutual independence. The general scheme of the worksheet is shown in Table III. In the first column, each parameter, x_i , is entered and at the bottom of that column the result, y , is computed in a single cell. This column is then copied across n columns with n equal to the number of parameters, x_i . The standard uncertainty for each parameter, $u(x_i)$, is entered above each column and then added to each x_i along the diagonal. The addition of the standard deviation produces a small change in y which is computed by differencing the result from column 'i' with the result from the first or left most column. The partial derivative of y with respect to x_i appears in this result. Further computation of the sensitivity coefficients and the expanded uncertainty is a straightforward use of the formula capability of the spreadsheet program to compute Equations (14) and (13), respectively. Table IV further demonstrates the numerical method with some nominal values for

Table III. General example of Kragten spreadsheet.

Base computation of y	Numerical differentiation			
	$u(x_1)$	$u(x_2)$...	$u(x_n)$
x_1	$x_1 + u(x_1)$	x_1	x_1	x_1
x_2	x_2	$x_2 + u(x_2)$	x_2	x_2
\vdots	\vdots	\vdots	\vdots	\vdots
x_n	x_n	x_n	x_n	$x_n + u(x_n)$
y	$y + \frac{\partial y}{\partial x_1} u(x_1)$	$y + \frac{\partial y}{\partial x_2} u(x_2)$...	$y + \frac{\partial y}{\partial x_n} u(x_n)$
Δy_i	$\frac{\partial y}{\partial x_1} u(x_1)$	$\frac{\partial y}{\partial x_2} u(x_2)$...	$\frac{\partial y}{\partial x_n} u(x_n)$
s_i	$\frac{\partial y}{\partial x_1} \frac{x_1}{y}$	$\frac{\partial y}{\partial x_2} \frac{x_2}{y}$...	$\frac{\partial y}{\partial x_n} \frac{x_n}{y}$
	$\left(\frac{u_c(y)}{y}\right)^2 = s_1^2 \left(\frac{u(x_1)}{x_1}\right)^2 + s_2^2 \left(\frac{u(x_2)}{x_2}\right)^2 + \dots + s_n^2 \left(\frac{u(x_n)}{x_n}\right)^2$			

Table IV. Example of Kragten spreadsheet using nominal values.

Base computation of $\dot{q}_{\text{crctd,comp}}$	Numerical differentiation			
	$u(V_{\text{O}_2})=0.00002$	$u(C_{\text{bdp}})=0.00350$...	$u(D)=0.01$
$V_{\text{O}_2}=0.81799$ (V)	0.81801	0.81799	0.81799	0.81799
$C_{\text{bdp}}=0.0698$ (m ³ /Kkg)	0.0698	0.0733	0.0698	0.0698
...
$D=1.52$ (m)	1.52	1.52	1.52	1.53
$\dot{q}_{\text{crctd,comp}}=0.6237$ (MW)	0.6225	0.6550	...	0.6320
$\Delta \dot{q}_{\text{crctd,comp}}$ (MW)	-0.0012	0.0313	...	0.0083
s_i	80.2	1.0	...	2.0
	$\left(\frac{u_c}{\dot{q}_{\text{crctd,comp}}}\right)^2 = 80.2^2 \left(\frac{0.00002}{0.81799}\right)^2 + 1.0^2 \left(\frac{0.00350}{0.0698}\right)^2 + \dots + 2.0^2 \left(\frac{0.01}{1.52}\right)^2$			

computing heat release rate and their standard uncertainty. Details of the Kragten worksheet and its application to this example can be found in References [7, 14], respectively.

Each parameter input for Equations (4) and (5) was reduced to voltages, temperatures, and constants (universal and empirical). This increased the number of parameters by almost a factor of five. Each parameter and its corresponding standard uncertainty were input into the Kragten worksheet for each of the three fire sizes. The relative standard uncertainty and its corresponding sensitivity coefficient for some select parameters are listed in Table V for a nominally 0.65 MW natural gas fire. For the case of a fire generated from an unknown mixture of hydrocarbons, the generic constant of the heat produced for each unit mass of oxygen consumed must be applied. There is a greater uncertainty associated with this constant as demonstrated by the values in parentheses.

The product of the relative standard uncertainty and the non-dimensional sensitivity coefficient can be used as a first-order metric to identify parameters that may contribute significantly to the

Table V. Selected values and standard uncertainties of heat release rate measurement parameters for a nominally 0.65 MW natural gas fire (nominally 0.65 MW fire from an unknown mixture of hydrocarbon fuels).

Parameter (units)	Nominal value	$u(x_i)/x_i$	s_i	Uncertainty type
V_{O_2} (V)	0.81799	0.00003	80.2	A
$V_{O_2,Span}$ (V)	0.83297	0.00003	1.256	A
$X_{O_2,Span}$ (dimensionless)	0.2095	0.00239	1.261	B
$V_{O_2}^o$ (V)	0.83278	0.00003	0.514	A
V_{CO_2} (V)	0.237	0.01704	0.169	A
$V_{CO_2,Span}$ (V)	1.6293	0.00046	0.139	A
$X_{CO_2,Span}$ (dimensionless)	0.101	0.00500	0.139	B
$V_{CO_2}^o$ (V)	0.0335	0.01309	0.001	A
V_{CO} (V)	-0.0101	0.04726	0.004	A
$V_{CO,Span}$ (V)	2.2014	0.00029	0.000	A
$X_{CO,Span}$ (dimensionless)	0.0908	0.00500	0.000	B
RH (%)	45.0	0.04038	0.020	B
P_{amb} (torr)	754	0.00266	0.020	B
T_{amb} (°C)	30.0	0.05095	0.035	A
C_{bdp} (m ³ /K kg)	0.0698	0.05014	1.00	B
b_i (torr/V)	0.10	0.00000	0.083	B
$V_{bdp,i}$ (V)	1.81	0.06231	0.082	A
$T_{bdp,i}$ (K)	343.0	0.00466	0.010	A
D (m)	1.52	0.00661	2.007	B
$(\Delta H_c)_{Mass_O_2}^{HC}$ (MJ/kg O ₂)	12.55	0.00159	1.000	B
	(13.10)	(0.0267)	(1.000)	(B)
$(\Delta H_c)_{Mass_O_2}^{CO}$ (MJ/kg O ₂)	17.60	0.00057	0.000	B
α (dimensionless)	1.10	0.04364	0.019	A
$m_{V_{O_2}}$ (V/s) (constant)	-2.43×10^{-7}	0.00344	0.002	A
$j_{V_{O_2}}$ (V) (constant)	0.832475	0.00000	81.99	A
$m_{V_{CO_2}}$ (V/s) (constant)	9.09×10^{-7}	0.14630	0.000	A
$j_{V_{CO_2}}$ (V) (constant)	0.034387	0.00403	0.031	A
$m_{V_{CO}}$ (V/s) (constant)	-7.95×10^{-7}	0.71062	0.000	A
$j_{V_{CO}}$ (V) (constant)	-0.00536	0.02411	0.004	A
$u_c/\dot{q}_{cretd,comp}$		0.053 (0.059)		

combined uncertainty. Any parameter with a sensitivity coefficient greater than unity may potentially be a significant contributor. For this study, parameters with $s_i u(x_i)/x_i > 0.01$ are considered uncertainty contributors. These parameters are identified in Figure 4, which demonstrates that more than 95% of the uncertainty is determined by five parameters or fewer: oxygen voltage, carbon dioxide voltage, duct diameter, the generic constant for the heat produced per unit mass of oxygen consumed, and the bi-directional probe constant. For the case of a known fuel composition, the constant for heat produced per unit mass of oxygen consumed can be precisely determined and therefore the uncertainty contribution of this term is small. The uncertainty associated with this

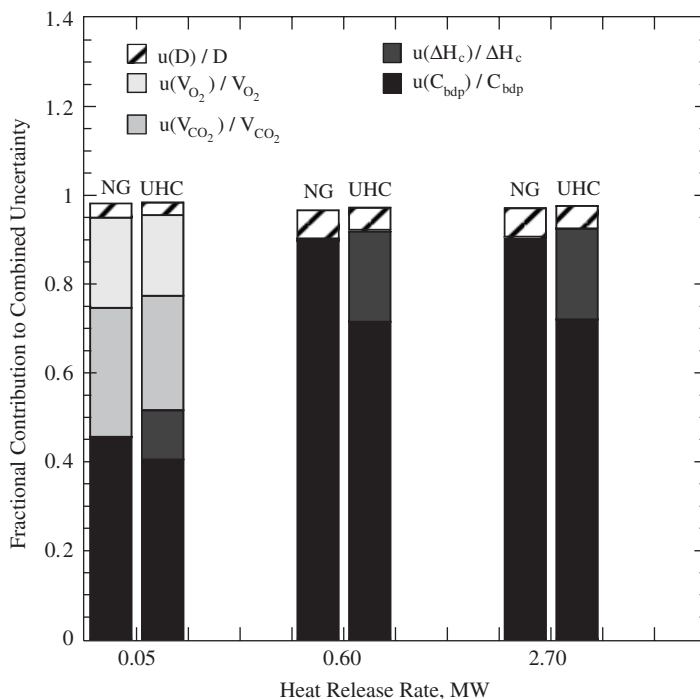


Figure 4. Parameters with significant uncertainty contribution (natural gas fire—NG, unknown hydrocarbon fire—UHC).

term is almost negligible for natural gas but not so for fuels containing unknown mixtures of hydrocarbons.

The oxygen and carbon dioxide voltages are utilized to compute the difference from ambient levels. As demonstrated in the previous example, the uncertainty due to the signal noise may have a significant effect when the differences are very small. Computing the mass flow rate of air in the exhaust stream requires determining the area of the exhaust duct which is proportional to the square of its diameter. The squared term results in a sensitivity coefficient of 2, therefore amplifying the uncertainty of the measurement of the exhaust duct diameter. The uncertainty of the empirically determined bi-directional probe constant is relatively large and 100% ($s_i = 1.0$) of it is contributed to the combined uncertainty over the entire range of heat release rate.

For the case of a fire generated from an unknown mixture of hydrocarbon fuels, the uncertainty of the method to compute heat release rate by oxygen consumption calorimetry is ultimately limited by the uncertainty of the generic constant for heat produced per unit mass of oxygen consumed. Efforts to reduce the combined uncertainty should concentrate on reducing the uncertainty of the two parameters used in the computation of exhaust mass flow rate, duct diameter, and bi-directional probe constant. Exploring independent methods of exhaust duct mass flow rate measurement with less uncertainty should also be considered.

Multiple tests were conducted over a period of two days to quantify the repeatability of the procedure to measure the heat release rate. The experiments included both the heat input measurement and the calorimetry measurement. Repeat measurements were conducted at six separate

Table VI. Absolute combined uncertainty, standard deviation, and relative expanded uncertainty for a natural gas fire.

Nominal HRR (MW)	Heat input measurement			Heat release rate measurement		
	u_c (MW)	σ (MW)	$U_c/\dot{q}_{\text{burner}}$	u_c (MW)	σ (MW)	U_c/\dot{q}
0.05	0.0006	0.0028	0.115	0.0038	0.0057	0.273
0.65	0.0078	0.0026	0.025	0.0345	0.0098	0.110
2.70	0.0324	0.0172	0.027	0.1431	0.0228	0.107

conditions: three heat input set points at two exhaust flow conditions. The standard deviation of the repeat measurements, σ , was used to estimate a standard uncertainty for the process of conducting the measurement. Precisely repeating the process of large-scale heat release rate measurements is not trivial due to the complexity of the facility, the number of operators, and the conditions that may influence the facility.

The revised combined uncertainty, u'_c , was computed by adding in quadrature the combined uncertainty from the uncertainty propagation and the standard deviation of the repeat measurements:

$$u'_c = \sqrt{u_c^2 + \sigma^2} \quad (20)$$

Finally, the expanded uncertainty, U_c , was computed as $2u'_c$, ($k=2$). The uncertainty estimates for the measured heat input and the measured heat release rate are presented in Table VI. Ideally the standard deviation is an estimate of the combined uncertainty; therefore, the uncertainty as computed in Equation (20) is a conservative estimate due to some level of double counting the uncertainty. Sources of uncertainty not included in the model equation of measured heat release rate such as operator error, environmental conditions, or undetected equipment failures are now estimated by the standard deviation of the repeat measurements. Computing the combined uncertainty in this manner is a first-order estimate that addresses some of the random sources of error which are not represented in the equation modeling the heat release rate measurement.

The uncertainty estimates for the heat release rate measurement (calorimeter) are for a fire from a well-characterized fuel (natural gas) where the uncertainty of the heat of combustion term is small. In the case that the fuel is not well characterized, such as an item of furniture, the uncertainty of the heat of combustion term will increase and the expanded relative uncertainty of the heat release rate measurement is estimated to increase by a factor of 1.02 (at low heat release) to 1.11 (at high heat release rate).

5. MEASUREMENT PERFORMANCE

Two very practical results of conducting a detailed uncertainty analysis are the creation of a tool for quality control and a benchmark level for system performance evaluation. Figure 5 is an example of the performance of the heat release rate measurement facility over an operational period of 19 months. The measurements of heat input into the facility and the heat released into the exhaust are simultaneous and independent measurements. Ideally the ratio of the two measurements should be unity. This comparison of simultaneous and independent measurements of the same process is another gauge of facility performance. Using known heat inputs is recommended for

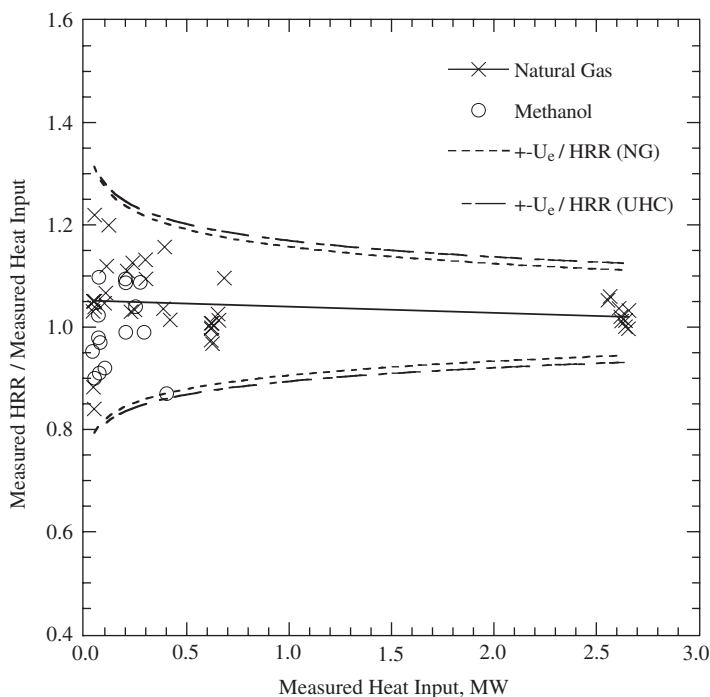


Figure 5. Heat release rate (HRR) measurement facility performance and quality control curve.

the confirmation and not the calibration of large-scale heat release rate facilities. When burners are used to calibrate heat release rate measurement facilities, the uncertainty of the heat release rate measurement is then tied to the uncertainty in the ability to measure the heat output of the burner. Therefore, the heat release rate measurement by oxygen consumption calorimetry is not independent of the heat input measurement. Heat input measurements of a given burner may rely on assumptions such as complete combustion and estimates of fuel heat content based on historical averages of fuel composition. Unless measurements to support or eliminate these assumptions are also conducted, it is unwise to use heat input measurements as bias corrections to heat release rate measurements and ultimately increase the uncertainty of the latter. This work demonstrates that, independent of a heat input calibration, it is possible to conduct a very good measurement of heat release rate by oxygen consumption calorimetry through good procedural calibrations of each instrument and a good characterization of the measurement facility.

The uncertainty of the heat input measurement, presented in Table VI, ranges from 2 to 4 times less than the uncertainty of the measurement of heat released. The relative discrepancy between the two measurements falls within the band of relative uncertainty for the heat release rate measurement. The greatest discrepancy and the greatest uncertainty occur when oxygen depletion and carbon dioxide production are low and the uncertainties of these measurements are amplified. In the case of large fires, the oxygen depletion and carbon dioxide production are large. The uncertainty of the heat release rate measurement appears to be dominated by the uncertainty of the measurement of mass flow rate in the exhaust, specifically the measurement of gas velocity and duct diameter. As shown in Figure 5, a power law fit of the uncertainty estimates (dashed curves)

provides a tool for easily estimating the uncertainty of any measurement from the facility. The curves also provide banding for quality control. For example, if during independent confirmation measurements with a known heat input the discrepancy between the heat input measurement and the heat release rate measurement falls outside of the uncertainty bands, the measurements should be designated as questionable. If the discrepancy continues to exist after repeat measurements, then an investigation into the cause of the discrepancy should begin.

6. CONCLUSIONS

The measurement uncertainty for a large-scale heat release rate facility was estimated by performing a detailed uncertainty audit of two independent measurements of the heating hazard potential due to fire: the heat input from a known fuel flowing through a burner and the heat release rate as a result of the burning of the fuel. Features of the uncertainty audit included: reducing the model equations down to their basic inputs of voltages, temperatures, and constants (empirical and universal) in order to guarantee that each measurement parameter is not mutually dependent upon another, performing a correction for instrument drift that may occur for long duration tests of fire retardant materials or configurations of materials with slow fire spread, estimating the uncertainty using a numerical method that can be easily applied in a computer spreadsheet, and attempting to reflect the uncertainty associated with procedure, operator, and facility malfunctions by combining the standard deviation of the repeat measurements with the combined uncertainty estimated from the uncertainty propagation.

The uncertainty propagation of the basic inputs demonstrated how to drill down to determine which measurements are most responsible for the combined uncertainty. In the case of the heat release rate described by Equation (4), the physical processes of the fire and the response of the facility are modeled, requiring a complex set of measurement inputs. This exercise provides better insight into how the measurement process actually takes place and whether the process reflects what is prescribed by the model. The uncertainty propagation of this model equation reveals that the uncertainty is mostly due to the uncertainty of the generic value for the heat produced per unit mass of oxygen consumed, and the uncertainty associated with determining the mass flow rate of the exhaust gases, specifically the uncertainty of the empirically determined constant for the bi-directional probes and the measurement of the duct diameter. At very low heat release rate where the oxygen depletion and carbon dioxide production are both small, the noise in the voltage measurements also contributes significantly to the uncertainty.

A method for correcting the heat release measurements for the instrument drift that may occur over long duration fire tests was demonstrated. The method assumes that measurement drift is linear, and a time history of the drift is estimated. Correcting heat release rate for measurement drift is recommended for evaluating the characteristics of peak heat release rate curves. This method is also useful for determining which instruments are most responsible for the overall drift in the measurement.

The relation converting measured values to heat release rate does not model the procedural steps followed by the operator(s), the skill of the operator(s), or the condition of the facility. The standard deviation for a series of measurements over a short period of time is a measure of how well the process was repeated. This value was used as an estimate of the uncertainty due to the factors mentioned. This is a reasonable estimate as demonstrated by the relative discrepancy

between measured heat input and measured heat release rate evaluated over a long period of time being within the uncertainty estimates.

A detailed uncertainty assessment as performed here provides a few simple tools. The curve fit of the relative expanded uncertainty can be used for quick estimates of the measurement uncertainty with respect to the heat release rate. The curve fit also sets a standard to work from for monitoring and improving performance as part of quality control efforts. However, as the facility changes due to modifications or as procedures change, the uncertainty assessment must be repeated to accurately reflect the changes.

NOMENCLATURE

α	combustion products expansion factor
ϕ	oxygen depletion factor
σ	standard deviation
D	exhaust duct diameter, m
F_d	fractional difference
ΔH_c	heat of combustion, MJ/kg (mass basis) or MJ/m ³ (volume basis)
j_i	intercept of drift correction for instrument i , V
m_i	slope of drift correction for instrument i , V/s
\dot{m}	rate of mass loss, kg/s
\dot{m}_e	mass flow rate in exhaust duct, kg/s
M_i	molecular weight of gas i , kg/kmol
P	gas pressure, Pa
\dot{q}	rate of heat released, MW or kW
RH	relative humidity
s_i	dimensionless sensitivity coefficient
t	time, s
T	gas temperature, K
$u(x_i)$	standard uncertainty for input quantity, x_i
$u_c(y)$	combined uncertainty for output quantity, y
U_e	expanded uncertainty
V_i	output voltage of instrument i , V
\dot{V}	volume flow rate, m ³ /s
X_i	volume fraction of exhaust gas i
X_i^o	volume fraction of ambient gas i

Subscripts

amb	measurement at ambient conditions
bdp	bi-directional probe
bkgd	background
comp	components
e	exhaust
i	species, instrument, etc.
NG	natural gas

ref reference temperature (300 K) and pressure (101 325 Pa)
Span measurement at the instrument span condition
sys system

REFERENCES

1. Axelsson J, Andersson P, Lonnermark A, VanHees P, Wetterlund I. Uncertainties in measuring heat and smoke release rates in the room/corner test and the SBI. *SP Report 2001:04*, SP Swedish National Testing and Research Institute, Boras, Sweden, 2001.
2. Sette B. Evaluation of uncertainty and improvement of the single burning item test method. *Ph.D. Thesis*, University of Ghent, Belgium, 2005.
3. Enright PA, Fleischmann CM. Uncertainty of heat release rate calculation of the ISO5660-1 cone calorimeter standard test method. *Fire Technology* 1999; **35**:153–169.
4. Yeager RW. Uncertainty analysis of energy-release rate measurement for room fires. *Journal of Fire Sciences* 1986; **4**:276–296.
5. Brohez S. Uncertainty analysis of heat release rate measurement from oxygen consumption calorimetry. *Fire and Materials* 2005; **29**:383–394.
6. Janssens ML. *Variability in Oxygen Consumption Calorimetry Tests*. American Society for Testing and Materials: Dallas, TX, 2002; 147–162.
7. Bryant RA, Ohlemiller TJ, Johnsson EL, Hamins A, Grove BS, Guthrie WF, Maranghides A, Mulholland GW. The NIST 3 megawatt quantitative heat release rate facility. *NIST Special Publication 1007*, National Institute of Standards and Technology, Gaithersburg, MD, 2003.
8. Huggett C. Estimation of rate of heat release by means of oxygen-consumption measurements. *Fire and Materials* 1980; **4**:61–65.
9. Sensenig DL. Oxygen consumption technique for determining the contribution of interior wall finishes to room fires. *NBS/TN-1128*, NIST, Gaithersburg, MD, 1980.
10. Parker WJ. Calculations of the heat release rate by oxygen-consumption for various applications. *Journal of Fire Sciences* 1984; **2**:380–395.
11. Parker WJ, Janssens ML. *Oxygen Consumption Calorimetry, Heat Release in Fires*. Elsevier: New York, 1992; 31–59.
12. International Organization for Standardization. *Guide to the Expression of Uncertainty in Measurement*. Switzerland, 1995.
13. Kuyatt CE, Taylor BN. Guidelines for evaluating and expressing the uncertainty of NIST measurement results. *NIST/TN-1297*, NIST, Gaithersburg, MD, 1994.
14. Kragten J. Calculating standard deviations and confidence-intervals with a universally applicable spreadsheet technique. *Analyst* 1994; **119**:2161–2165.